

GSA Data Repository Item 2019171

Changes in landscape evolution patterns in the northern Alpine Foreland during the Mid-Pleistocene Revolution

Anne Claude¹, Naki Akçar¹, Susan Ivy-Ochs², Fritz Schlunegger¹, Peter W. Kubik², Marcus Christl², Christof Vockenhuber², Joachim Kuhlemann³, Meinert Rahn³ and Christian Schlüchter¹

¹*Institute of Geological Sciences, University of Bern, Baltzerstrasse 1-3, 3012 Bern, Switzerland
(anne.claude@geo.unibe.ch)*

²*Laboratory of Ion Beam Physics, ETH Zurich, Otto-Stern-Weg 5, 8083 Zurich, Switzerland*

³*Swiss Federal Nuclear Safety Inspectorate ENSI, Industriestrasse 19, 5200 Brugg, Switzerland*

Contents:

- Fig. DR1 Output of the depth profile modelling for Ängi site.**
- Fig. DR2 Probability density and cumulative distribution functions for Ängi site.**
- Fig. DR3 Age versus erosion rate plot for the Ängi ^{10}Be depth profile.**
- Fig. DR4 Output of the depth profile modelling for Rechberg site.**
- Fig. DR5 Probability density and cumulative distribution functions for Rechberg.**
- Fig. DR6 Age versus erosion rate plot for the Rechberg ^{10}Be depth profile.**
- Fig. DR7 Output of the ^{36}Cl depth profile modelling for Rechberg.**
- Fig. DR8 Frequency distribution plots resulting from ^{36}Cl modelling for Rechberg.**
- Fig. DR9 Age versus erosion rate plot for the Rechberg ^{36}Cl depth profile.**
- Fig. DR10 Output of the depth profile modelling for Irchel Steig site.**
- Fig. DR11 Probability density and cumulative distribution functions for Irchel Steig.**
- Fig. DR12 Age versus erosion rate plot for the Irchel Steig ^{10}Be depth profile.**
- Fig. DR13 Output of the depth profile modelling for Wilemer Irchel site.**
- Fig. DR14 Probability density and cumulative distribution functions for Wilemer Irchel.**
- Fig. DR15 Age versus erosion rate plot for the Mandach ^{10}Be depth profile.**
- Fig. DR16 Output of the depth profile modelling for Mandach site.**
- Fig. DR17 Probability density and cumulative distribution functions for Mandach.**
- Fig. DR18 Age versus erosion rate plot for the Mandach ^{10}Be depth profile.**
- Fig. DR19 Output of the depth profile modelling for Stadlerberg site.**
- Fig. DR20 Probability density and cumulative distribution functions for Stadlerberg.**
- Fig. DR21 Age versus erosion rate plot for the Stadlerberg ^{10}Be depth profile.**
- Table DR1 Major and trace element data of the samples from Rechberg**
- Table DR2 Input parameters for the ^{10}Be depth-profile modelling**
- Table DR3 Input parameters for the ^{36}Cl depth-profile modelling**
- Table DR4 Output values from the depth-profile modelling**
- Table DR5 Results of isochron-burial age simulations**

Introduction

This supporting information provides detailed information on the results of the depth-profile age calculations using Monte Carlo simulations, including 10 figures that are referenced but not included in the main article.

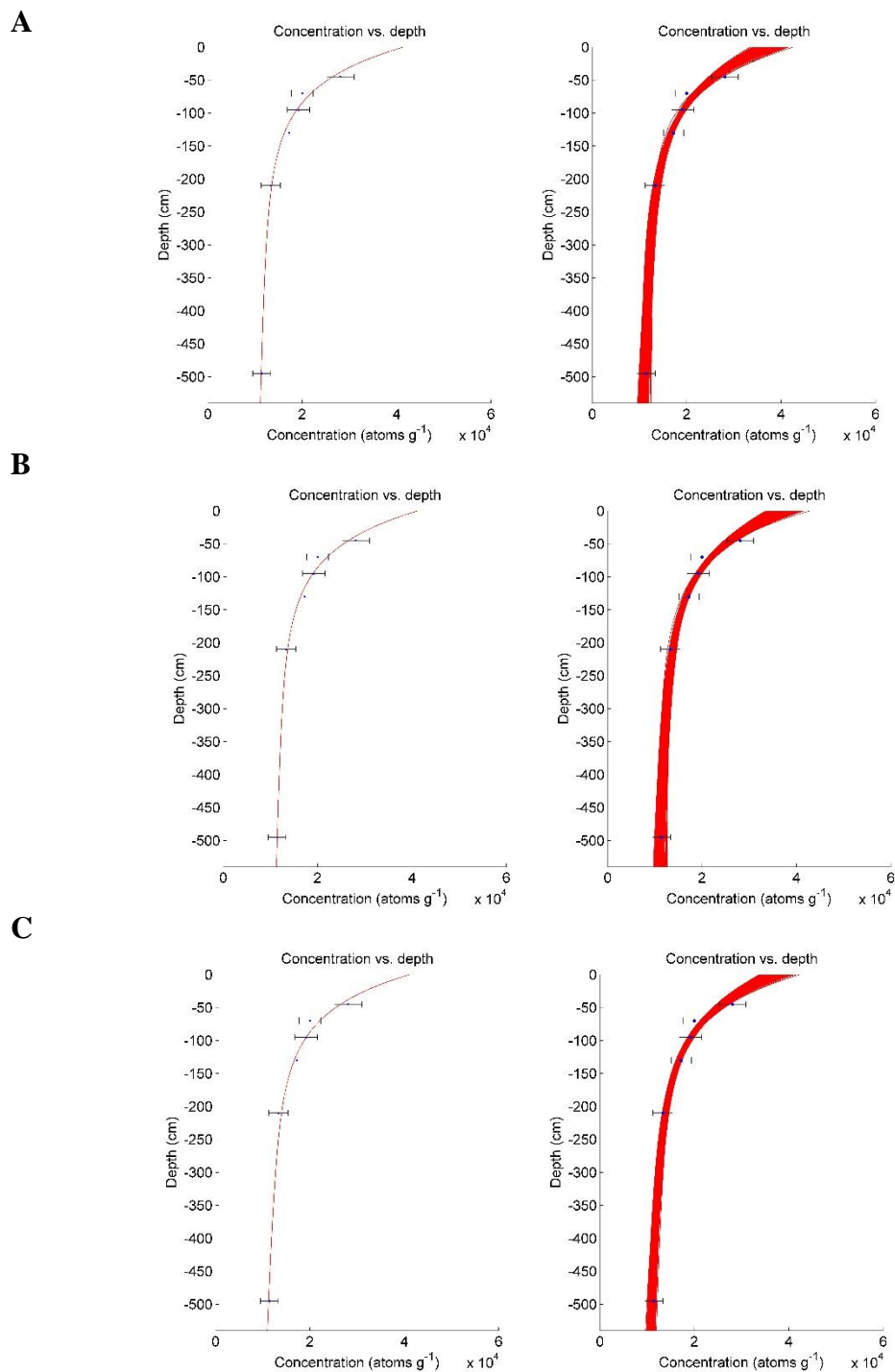


Fig. DR1 Depth profile output of the Monte Carlo age simulation for Ängi: Illustration of the best fit through the samples on the left; and 2σ solution space on the right. Error bars represent 2σ total measurement error. A: 0-150 m net erosion; B: -10-150 m net erosion; C: 100-150 m net erosion.

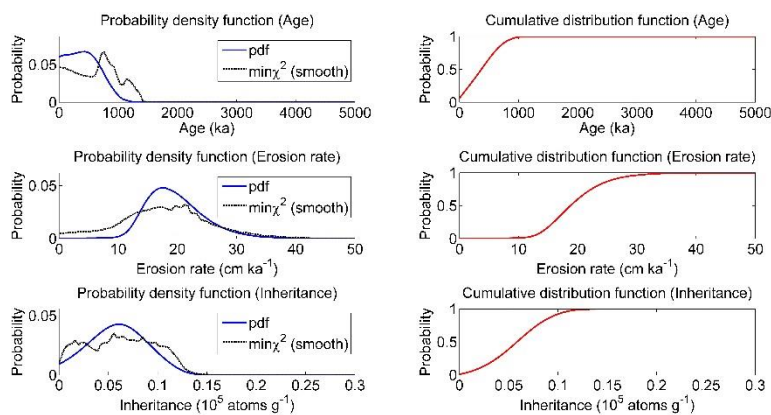
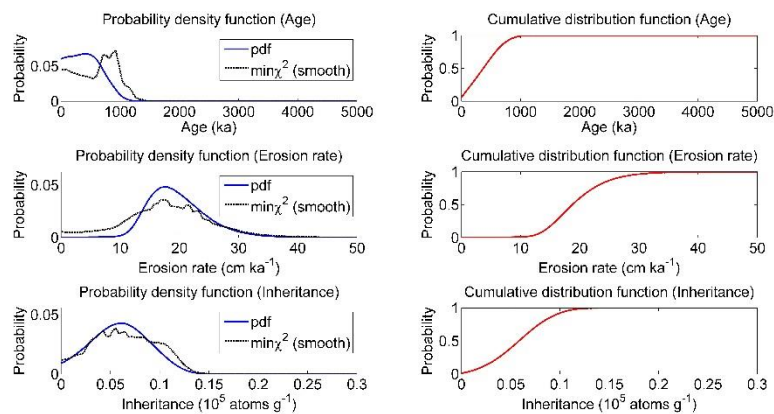
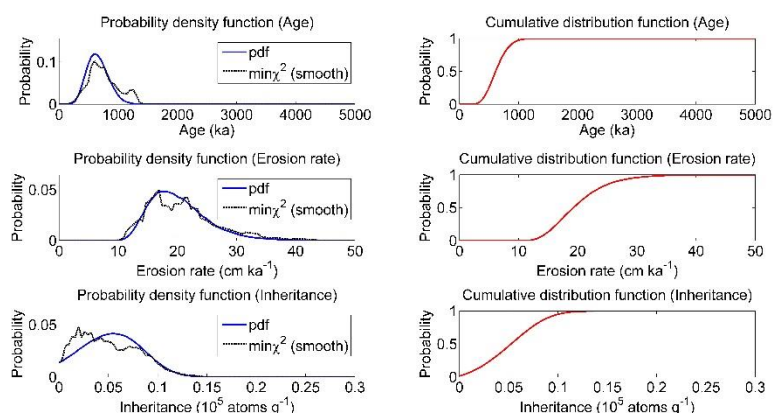
A**B****C**

Fig. DR2 Probability density and cumulative distribution functions for the 2σ age, erosion rate and inheritance solution spaces for the six ^{10}Be samples from Ängi. Solid black line indicates the lowest chi-square value. A: 0-150 m net erosion; B: -10-150 m net erosion; C: 100-150 m net erosion.

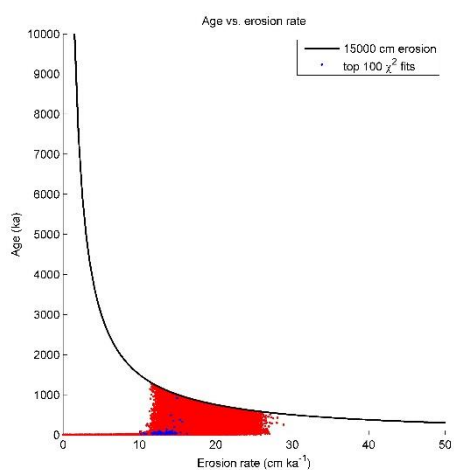
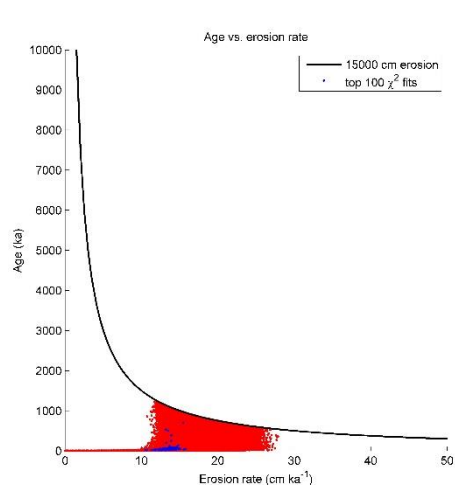
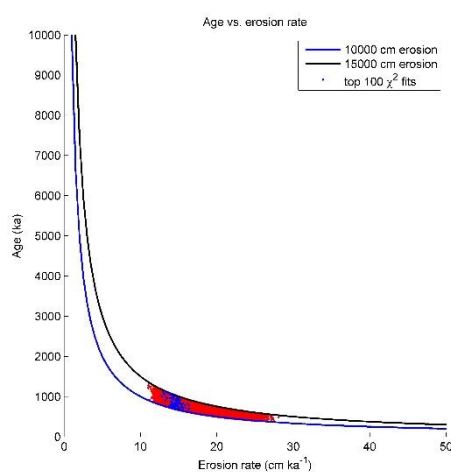
A**B****C**

Fig. DR3 Age versus erosion rate plot for the Ängi ^{10}Be depth profile. A: 0-150 m net erosion; B: -10-150 m net erosion; C: 100-150 m net erosion.

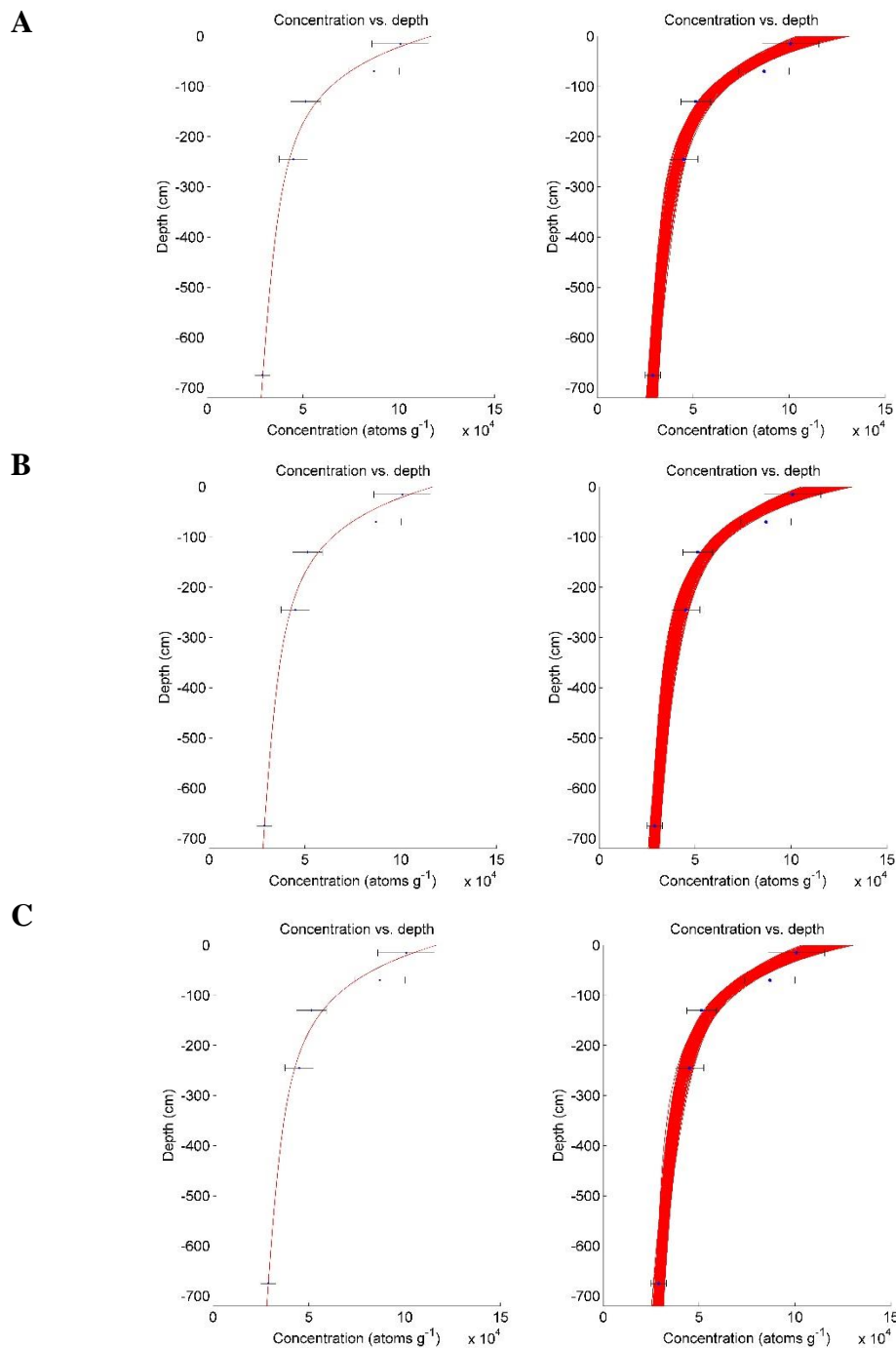


Fig. DR4 Depth profile output of the Monte Carlo age simulation for Rechberg: Illustration of the best fit through the samples on the left; and 3σ solution space on the right. Error bars represent 2σ total measurement error. A0 -28 m net erosion; B: -10-28 m net erosion; C: 10-28 m net erosion.

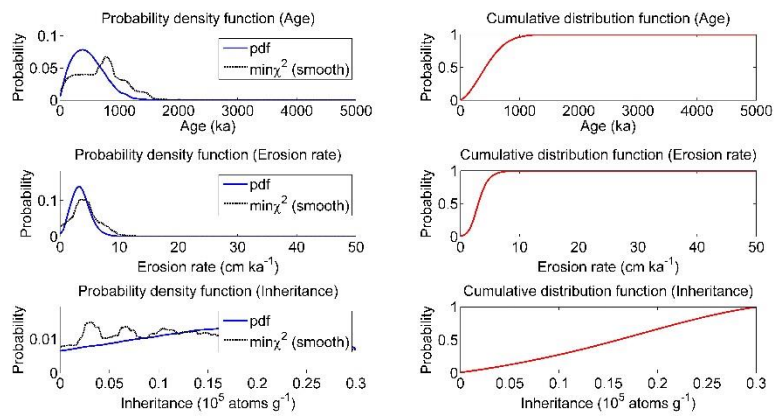
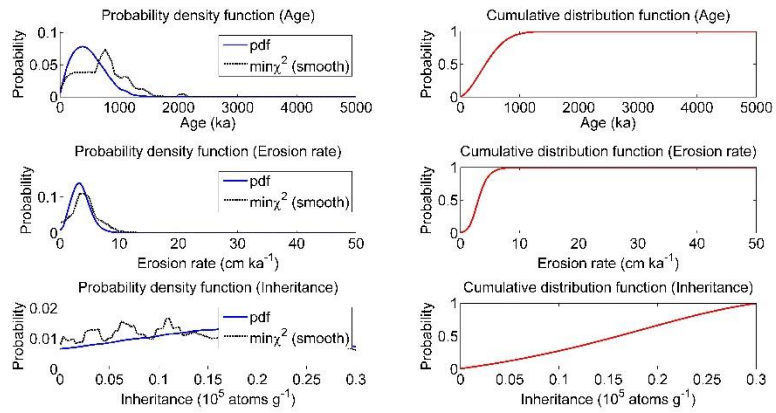
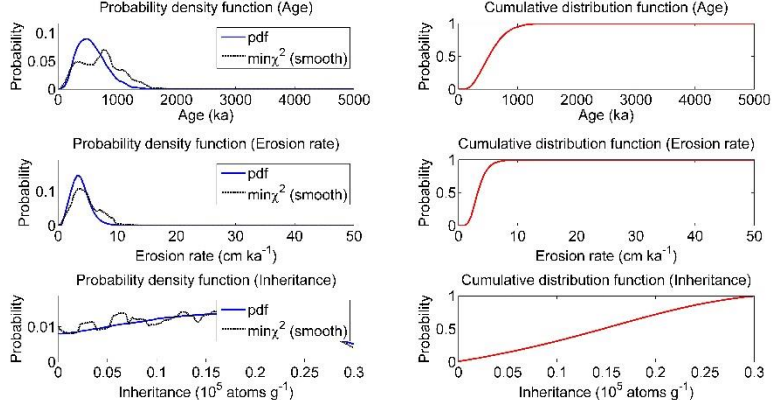
A**B****C**

Fig. DR5 Probability density and cumulative distribution functions for the 3σ age, erosion rate and inheritance solution spaces for ^{10}Be depth-profile from Rechberg. Solid black line indicates the lowest chi-square value. A: 0-28 m net erosion; B: -10-28 m net erosion; C: 10-28 m net erosion.

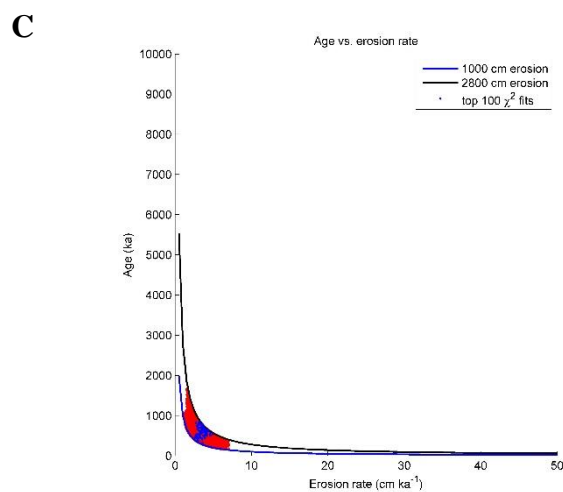
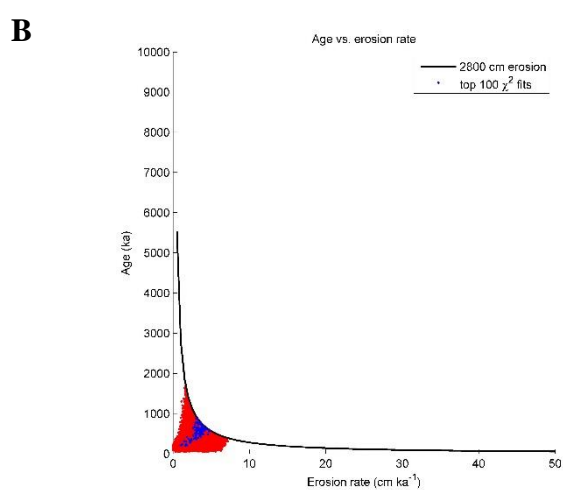
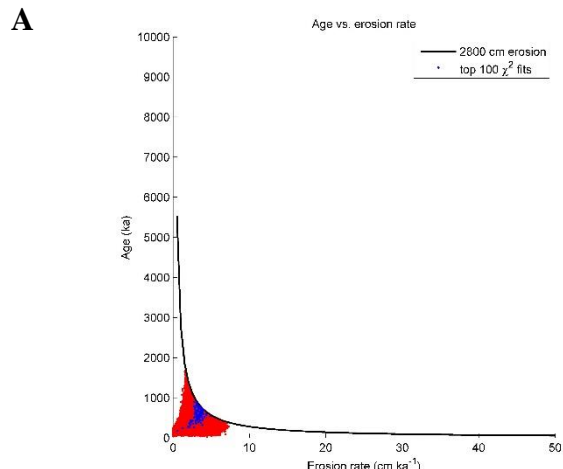
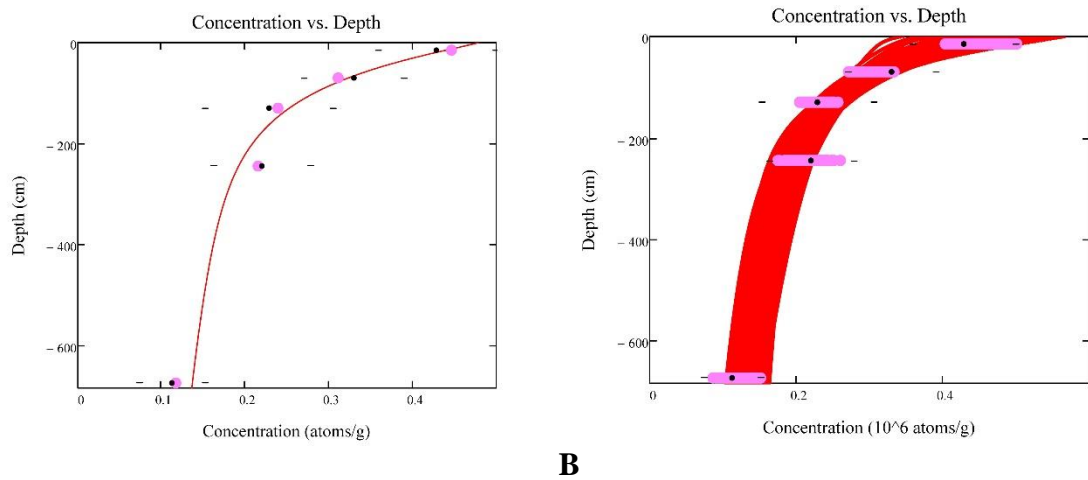


Fig. DR6 Age versus erosion rate plot for the Rechberg ^{10}Be depth profile. A: 0-28 m net erosion; B: -10-28 m net erosion; C: 10-28 m net erosion.



A

B

Fig. DR7 ^{36}Cl depth profile output of the Monte Carlo age simulation for Rechberg. A: Illustration of the best fit through the samples. B: 2σ solution space. Error bars represent 1σ total measurement error.

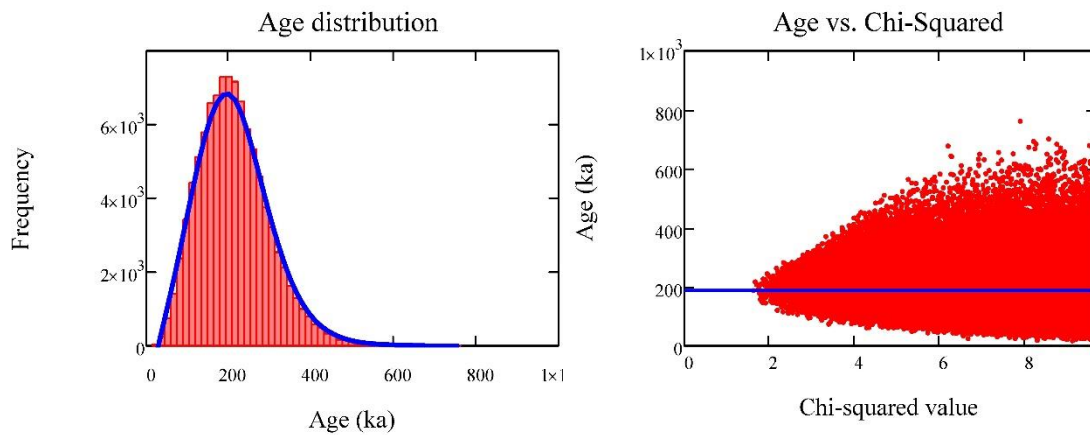
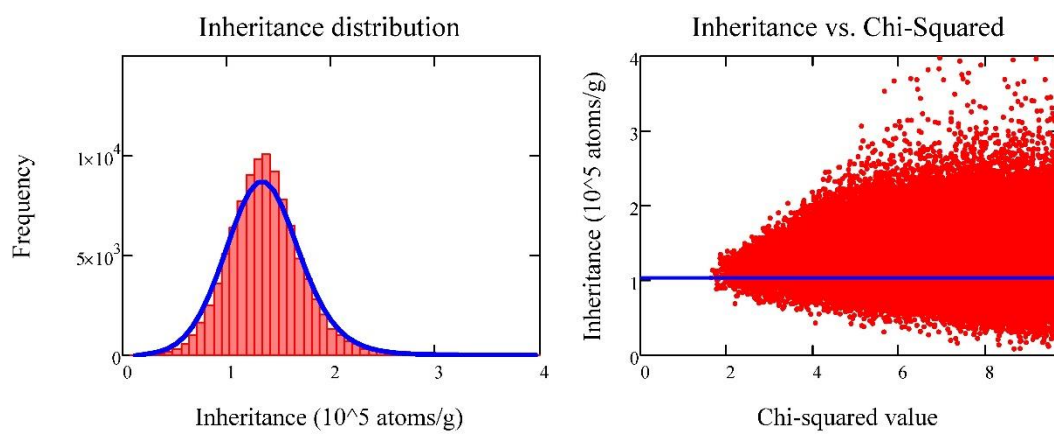
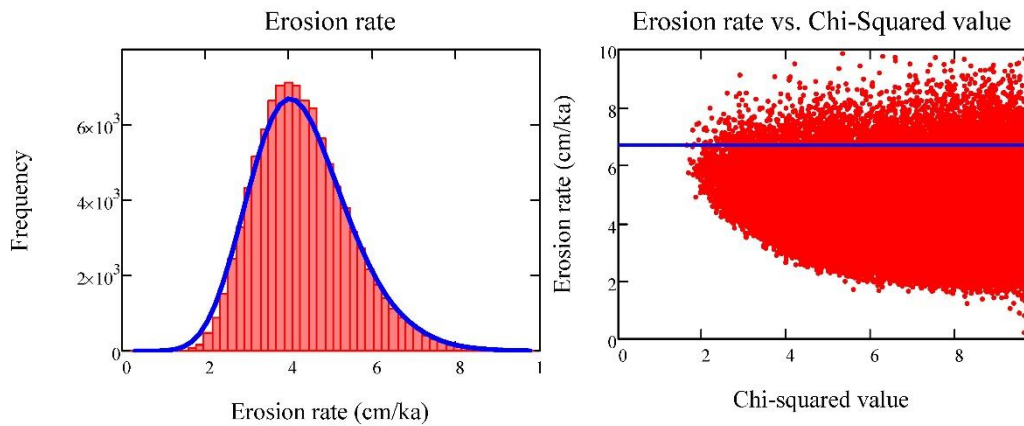
A**B****C**

Fig. DR8 Frequency distribution plots for the 2σ age, erosion rate and inheritance solution spaces for the five ^{36}Cl samples from Rechberg. Solid blue line indicates the lowest chi-square value.

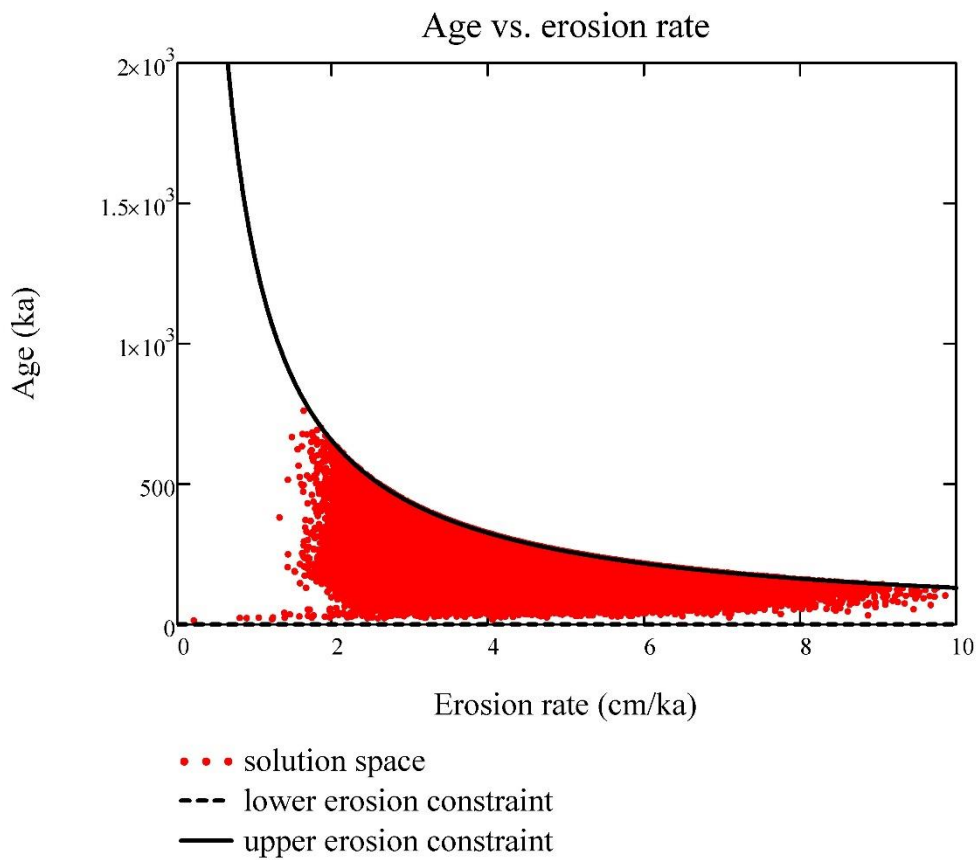


Fig. DR9 Age versus erosion rate plot for the Rechberg ^{36}Cl depth profile.

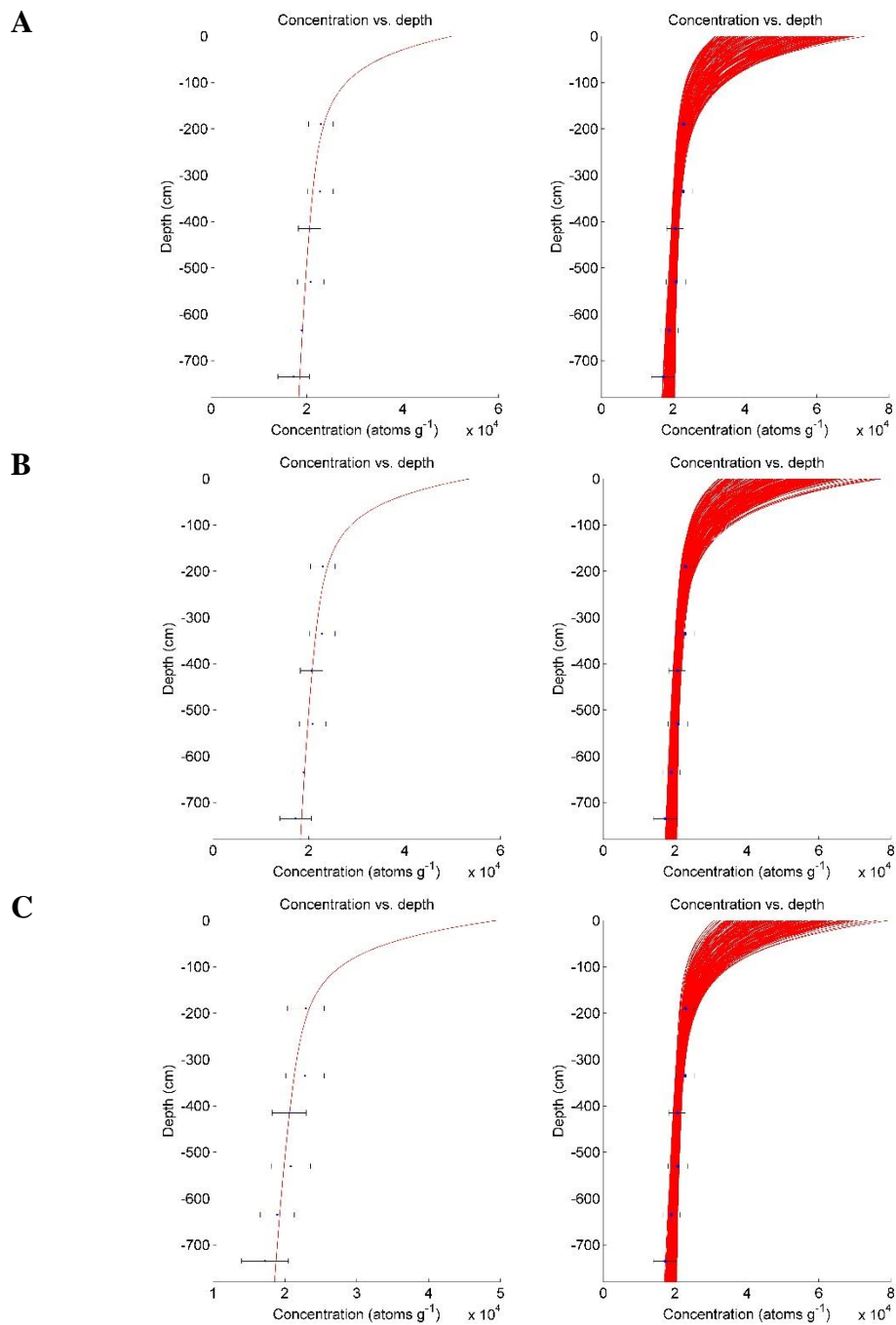


Fig. DR10 Depth profile output of the Monte Carlo age simulation for Irchel Steig:
 Illustration of the best fit through the samples on the left; and 2σ solution space on the right.
 Error bars represent 2σ total measurement error. A: 0-160 m net erosion; B: -10-160 m net
 erosion; C: 100-160 m net erosion.

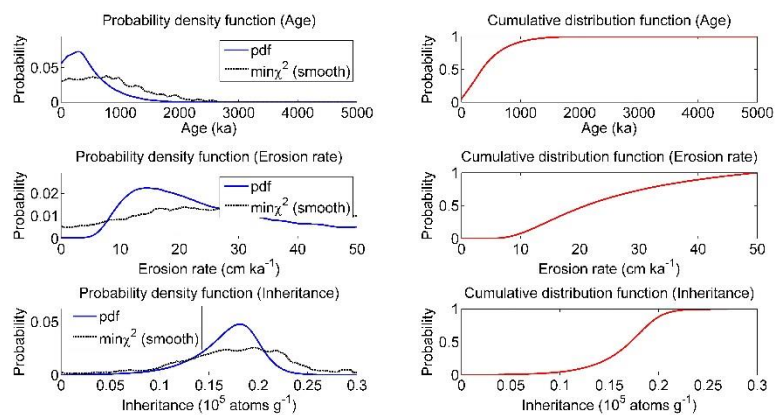
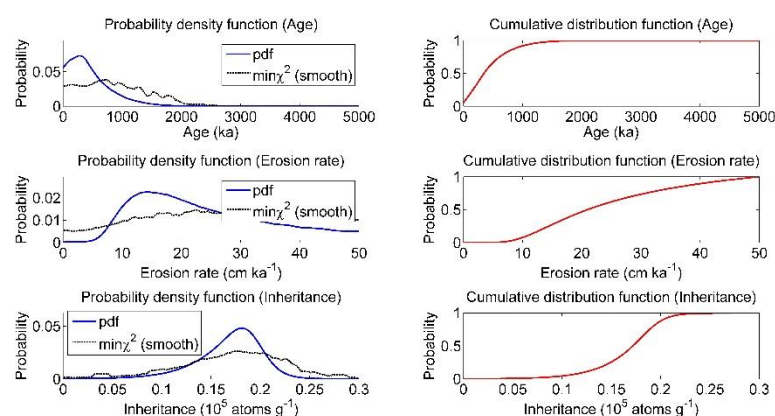
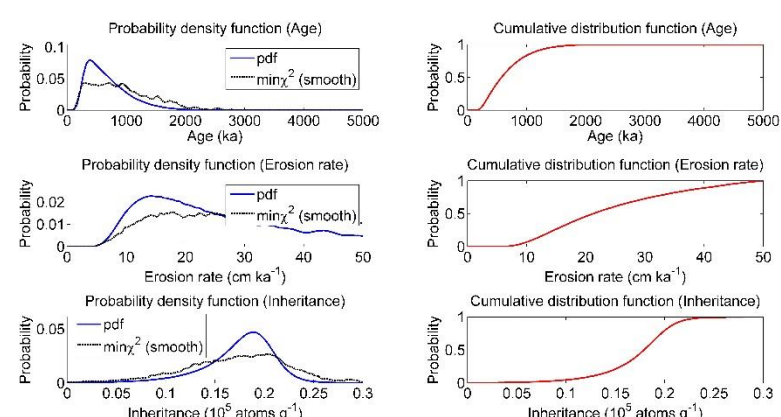
A**B****C**

Fig. DR11 Probability density and cumulative distribution functions for the 2σ age, erosion rate and inheritance solution spaces for ^{10}Be depth-profile from Irchel Steig. Solid black line indicates the lowest chi-square value. A: 0-160 m net erosion; B: -10-160 m net erosion; C: 100-160 m net erosion.

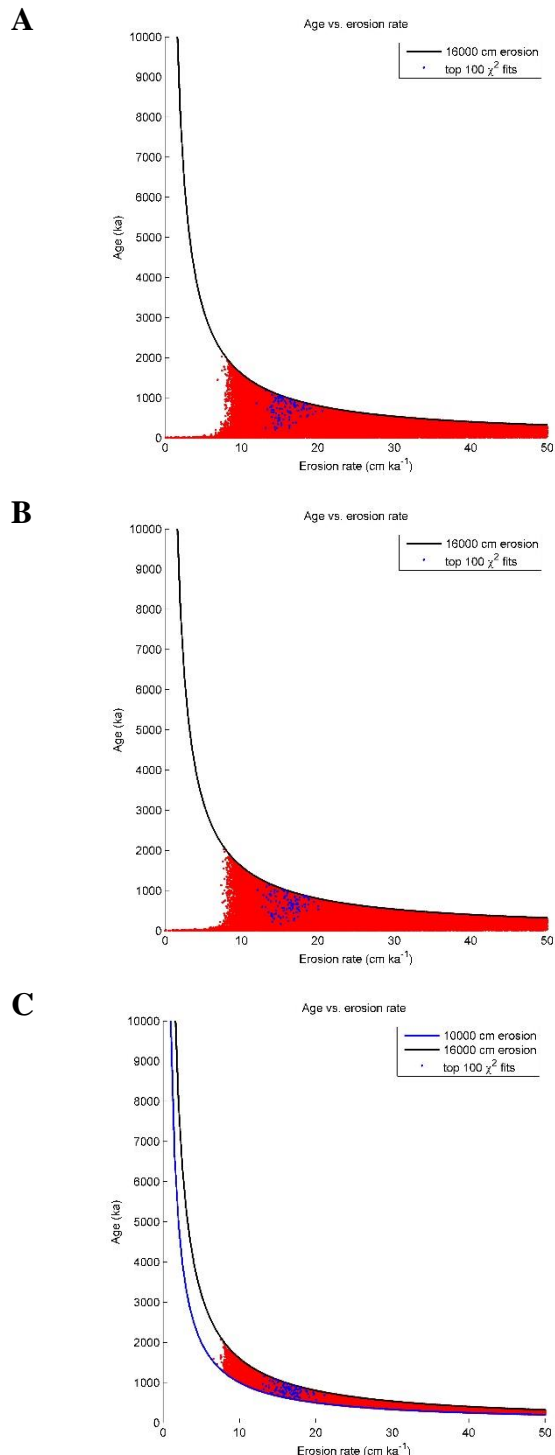


Fig. DR12 Age versus erosion rate plot for the Irchel Steig ^{10}Be depth profile. A: 0-160 m net erosion; B: -10-160 m net erosion; C: 100-160 m net erosion.

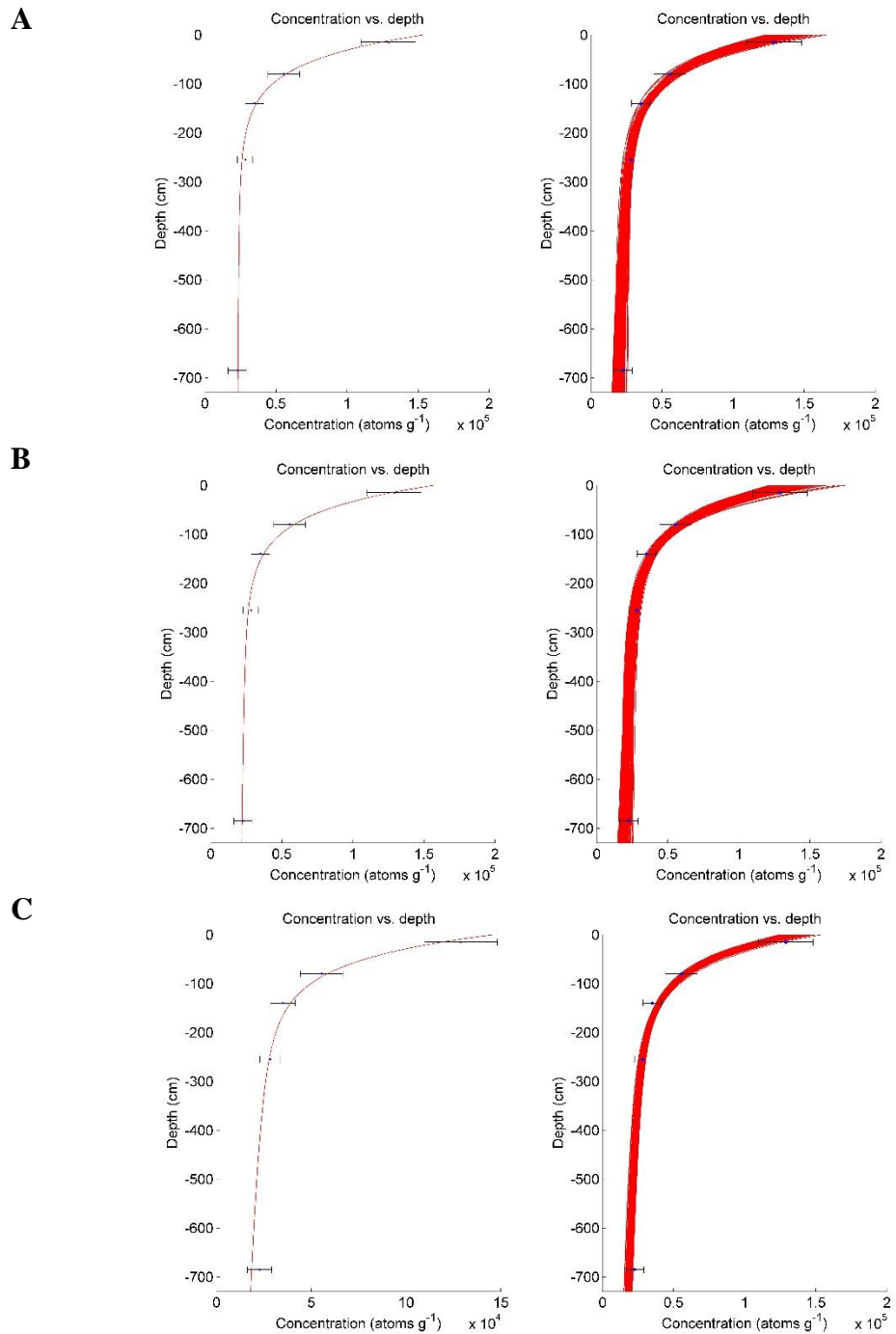


Fig. DR13 Depth profile output of the Monte Carlo age simulation for Wilemer Irchel: Illustration of the best fit through the samples on the left; and 4σ solution space on the right. Error bars represent 4σ total measurement error. A: 0-150 m net erosion; B: -10-150 m net erosion; C: 100-150 m net erosion.

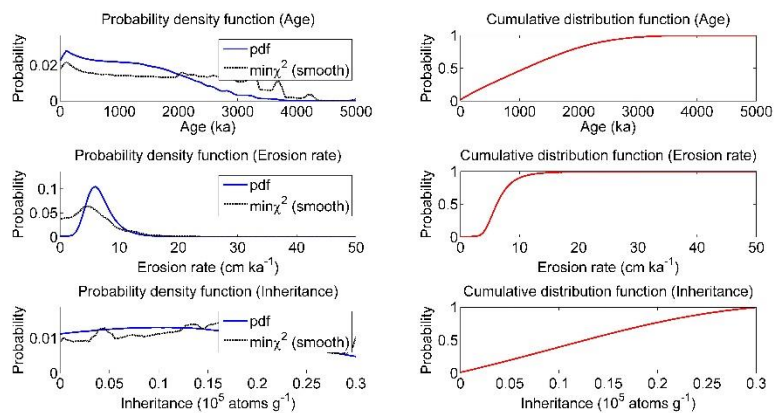
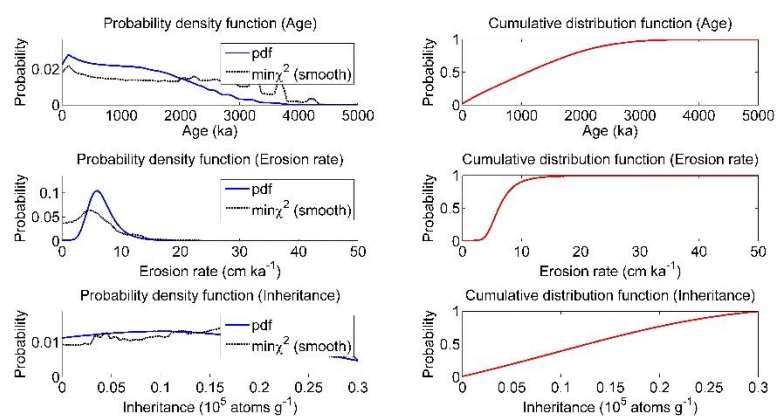
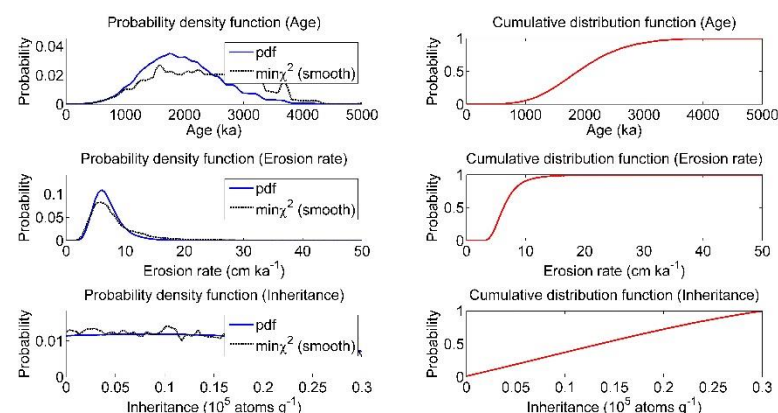
A**B****C**

Fig. DR14 Probability density and cumulative distribution functions for the 4σ age, erosion rate and inheritance solution spaces for ^{10}Be depth-profile from Wilemer Irchel. Solid black line indicates the lowest chi-square value. A: 0-150 m net erosion; B: -10-150 m net erosion; C: 100-150 m net erosion.

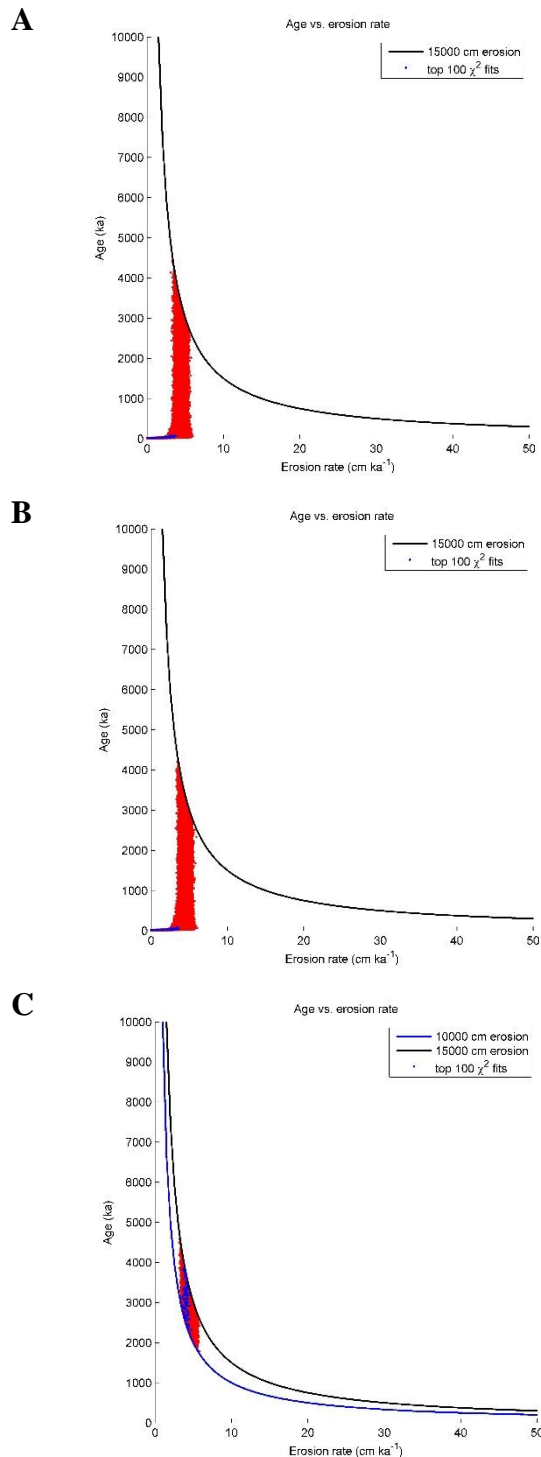


Fig. DR15 Age versus erosion rate plot for the Wilemer Irchel ^{10}Be depth profile. A: 0-150 m net erosion; B: -10-150 m net erosion; C: 100-150 m net erosion.

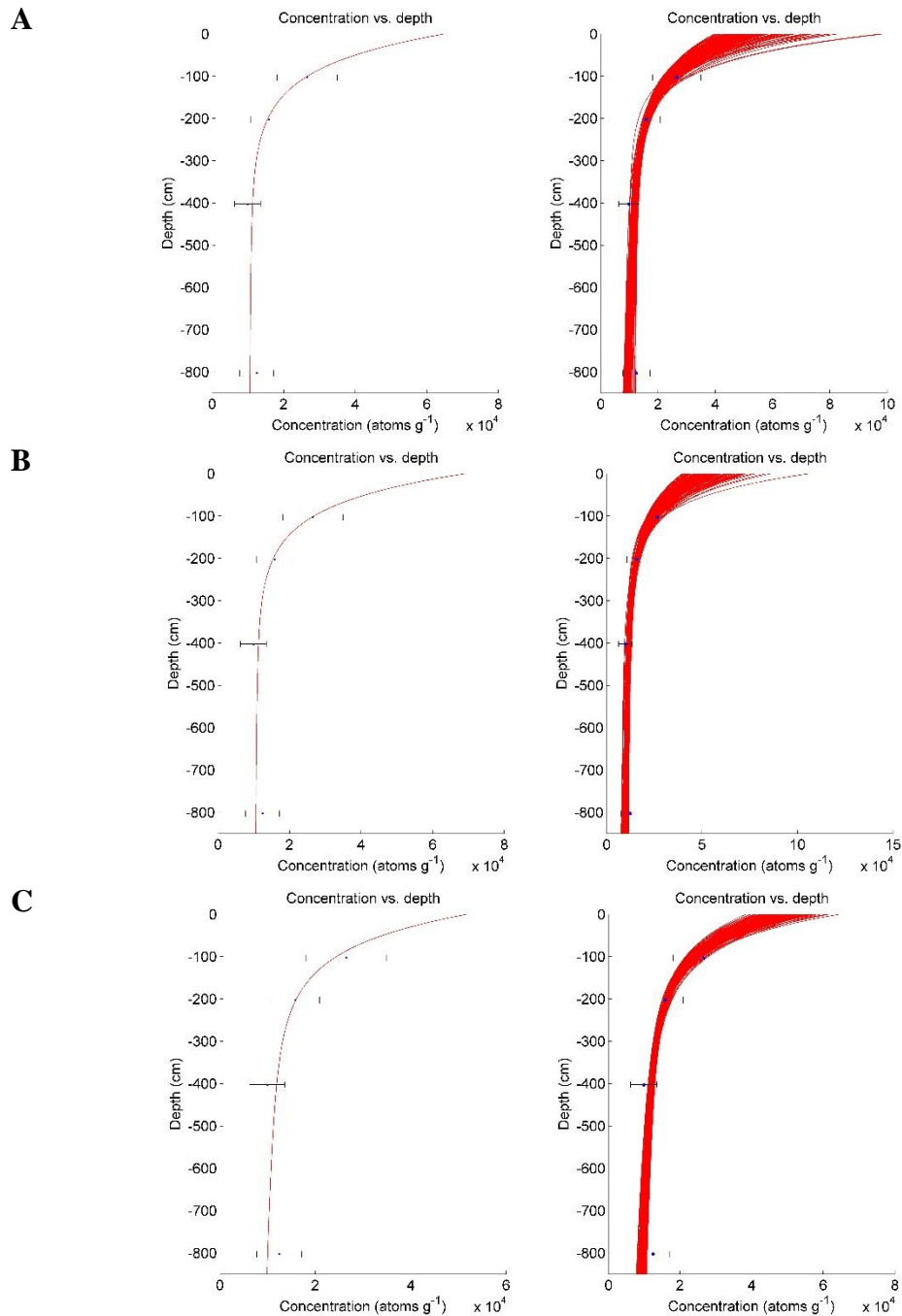


Fig. DR16 Depth profile output of the Monte Carlo age simulation for Mandach: Illustration of the best fit through the samples on the left; and 3σ solution space on the right. Error bars represent 2σ total measurement error. A0-150 m net erosion; B: -10-150 m net erosion; C: 100-150 m net erosion.

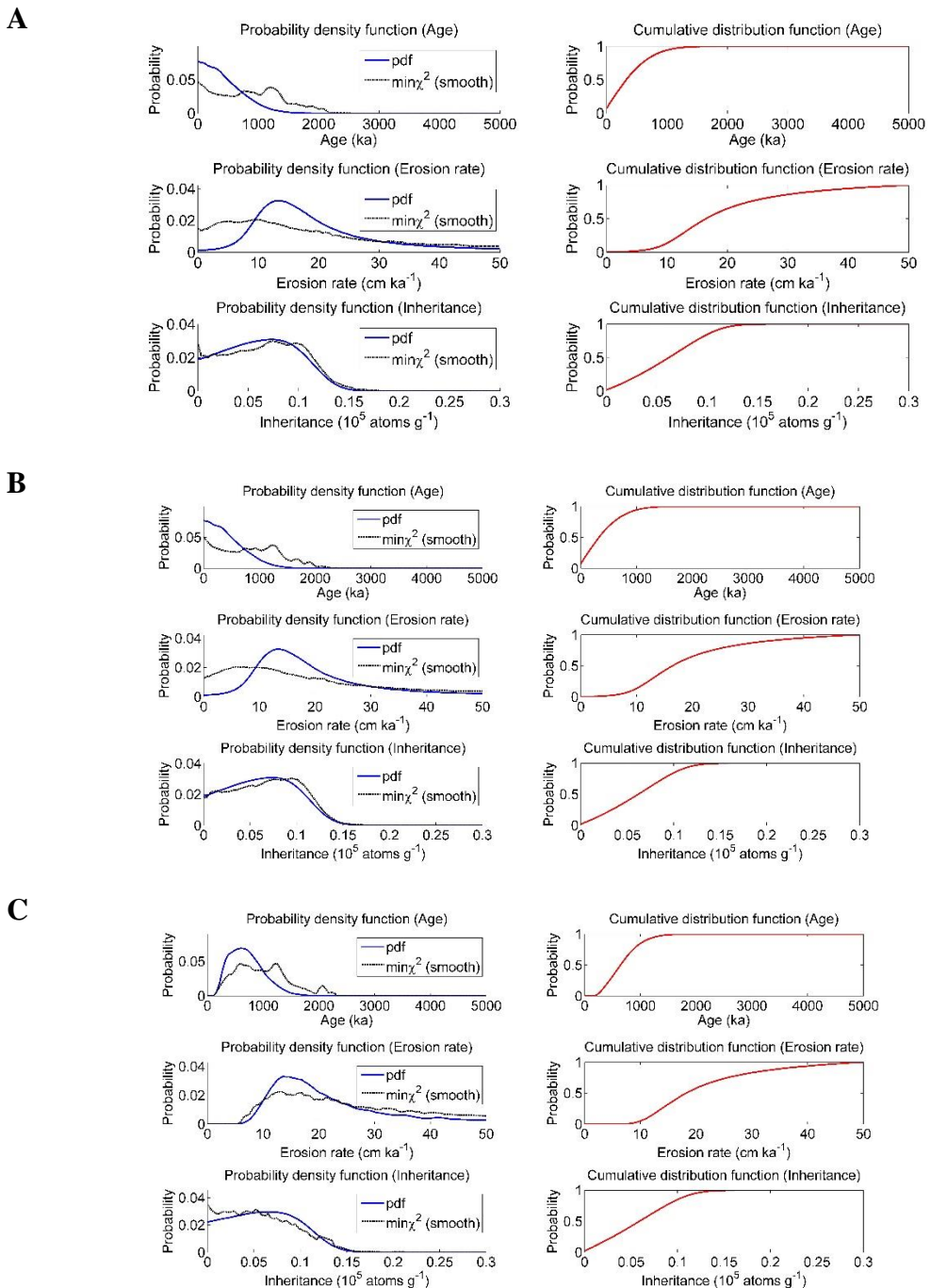


Fig. DR17 Probability density and cumulative distribution functions for the 3σ age, erosion rate and inheritance solution spaces for ^{10}Be depth-profile from Mandach. Solid black line indicates the lowest chi-square value. A: 0-150 m net erosion; B: -10-150 m net erosion; C: 100-150 m net erosion.

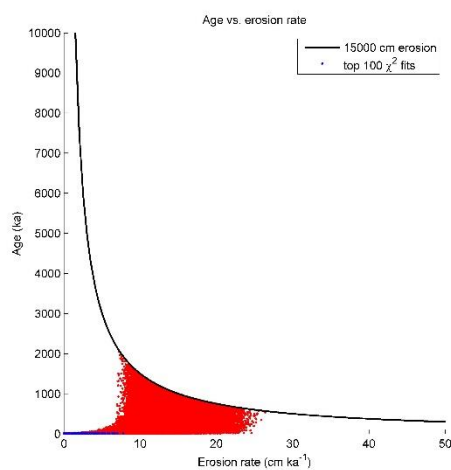
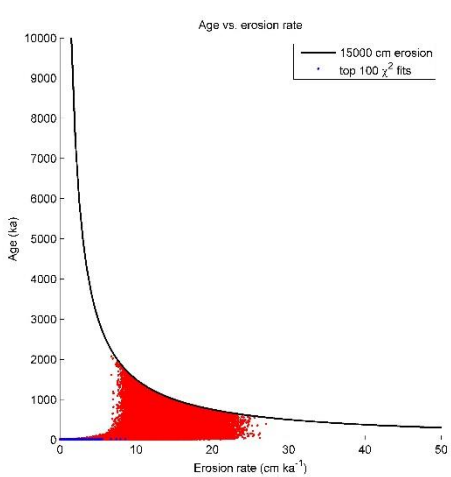
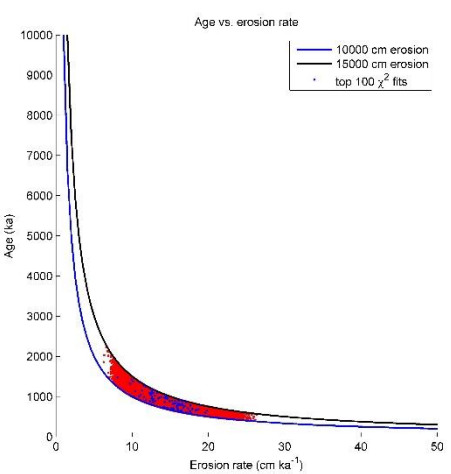
A**B****C**

Fig. DR18 Age versus erosion rate plot for the Mandach ^{10}Be depth profile. A: 0-150 m net erosion; B: -10-150 m net erosion; C: 100-150 m net erosion.

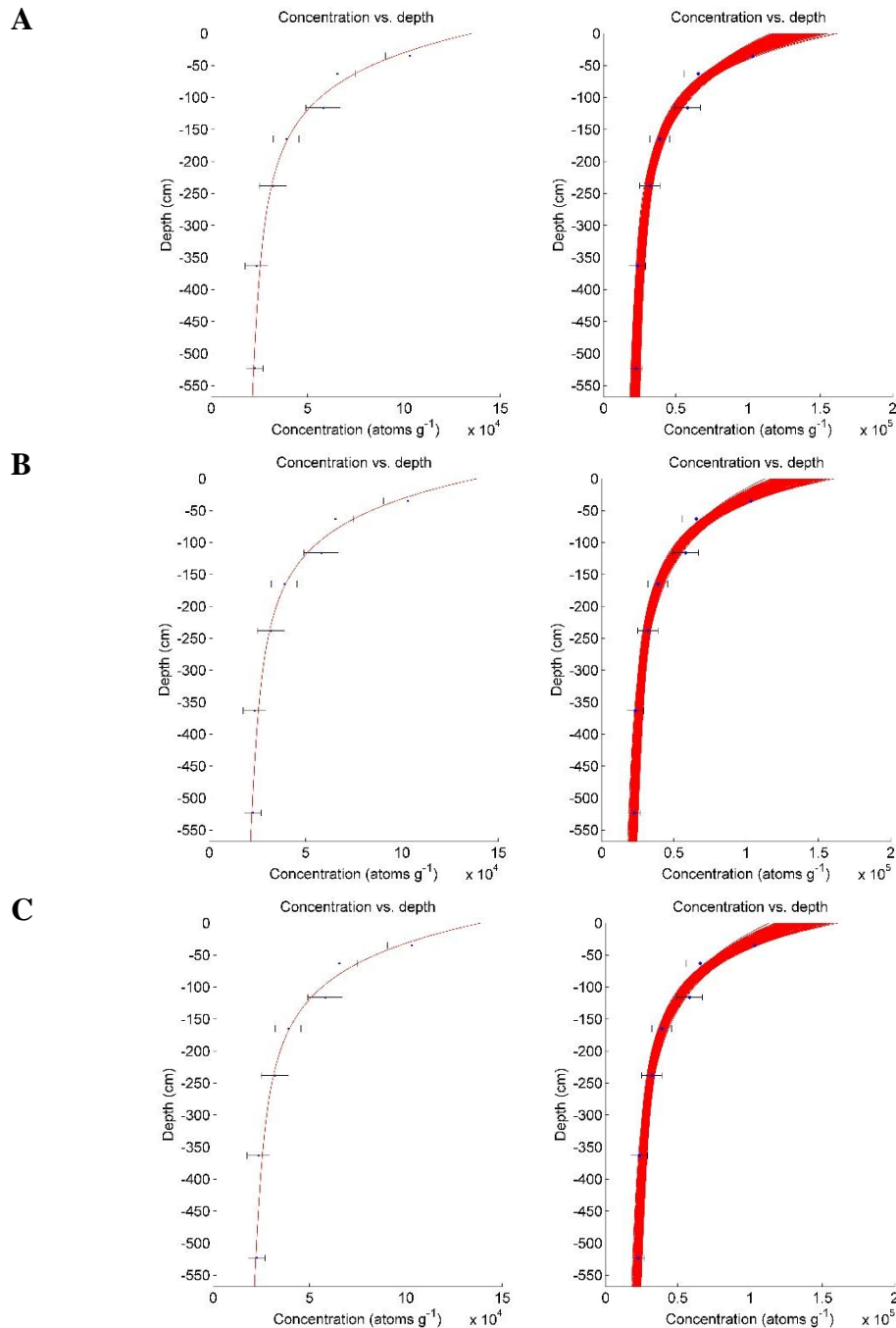


Fig. DR19 Depth profile output of the Monte Carlo age simulation for Stadlerberg:
 Illustration of the best fit through the samples on the left; and 3σ solution space on the right.
 Error bars represent 2σ total measurement error. A: 0-150 m net erosion; B: -10-150 m net
 erosion; C: 100-150 m net erosion.

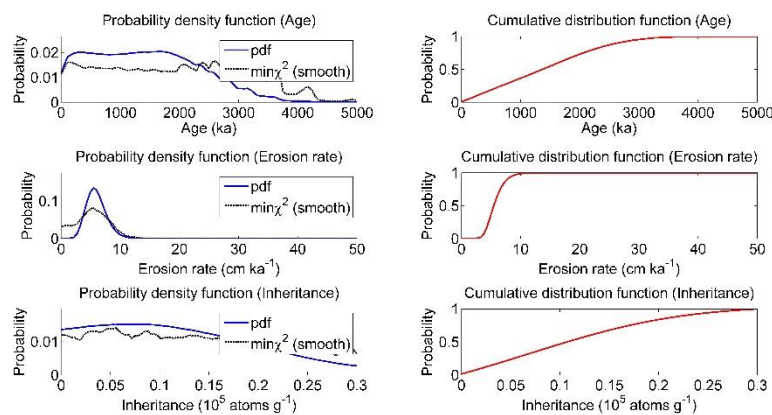
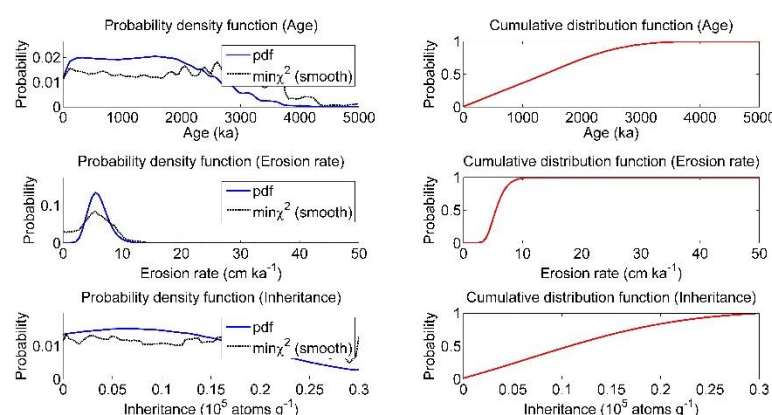
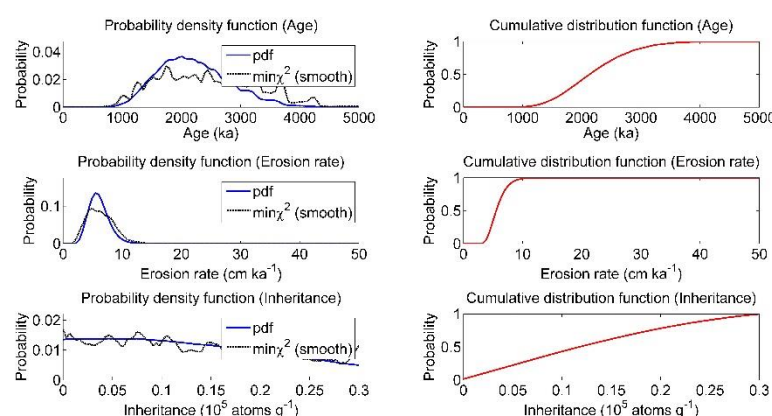
A**B****C**

Fig. DR20 Probability density and cumulative distribution functions for the 3σ age, erosion rate and inheritance solution spaces for ^{10}Be depth-profile from Stadlerberg. Solid black line indicates the lowest chi-square value. A: 0-150 m net erosion; B: -10-150 m net erosion; C: 100-150 m net erosion.

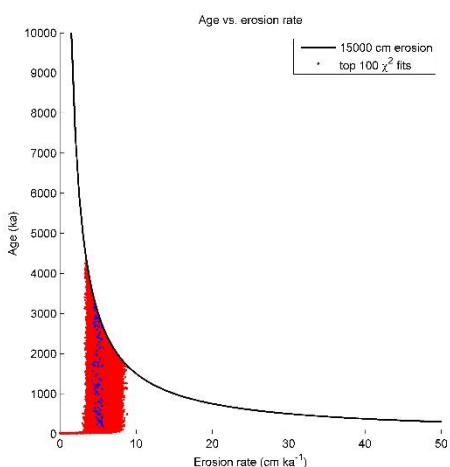
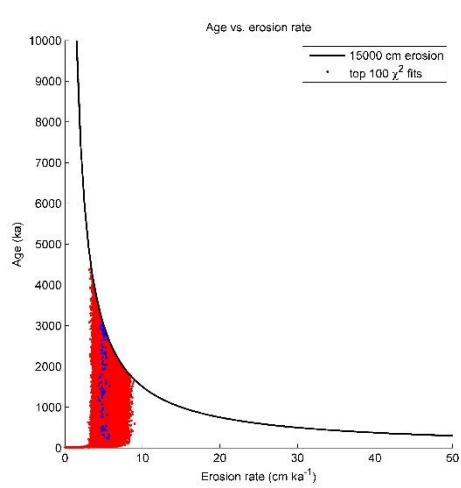
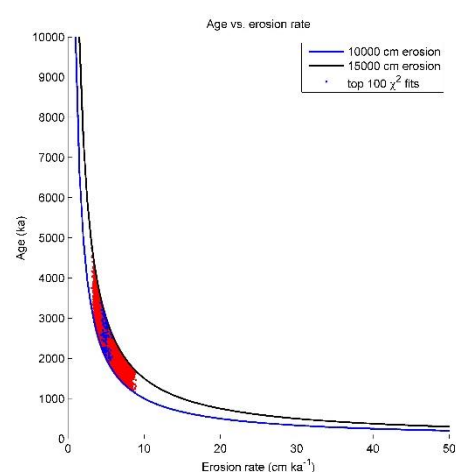
A**B****C**

Fig. DR21 Age versus erosion rate plot for the Stadlerberg ^{10}Be depth profile. A: 0-150 m net erosion; B: -10-150 m net erosion; C: 100-150 m net erosion.

TABLE DR1. MAJOR AND TRACE ELEMENT DATA (DETERMINED BY XRAL, ONTARIO, CANADA) OF THE SAMPLES FROM RECHBERG

Sample name	SiO ₂ (wt.%)	Al ₂ O ₃ (wt.%)	Fe ₂ O ₃ (wt.%)	MnO (wt.%)	MgO (wt.%)	CaO (wt.%)	Na ₂ O (wt.%)	K ₂ O (wt.%)	TiO ₂ (wt.%)	P ₂ O ₅ (wt.%)	Sm (ppm)	Gd (ppm)	U (ppm)	Th (ppm)
SCHW-DP-1b*	47.76	2.19	1.11	0.04	0.96	24.82	0.29	0.53	0.10	0.04	1.30	1.40	0.80	1.60
SCHW-DP-2	58.26	2.30	1.46	0.04	0.43	20.21	0.34	0.72	0.08	0.03	1.00	1.00	0.50	1.50
SCHW-DP-3b*	59.42	2.55	1.67	0.04	1.38	18.05	0.41	0.62	0.12	0.01	1.30	1.40	0.90	1.70
SCHW-DP-4b*	44.49	2.10	1.32	0.03	1.27	26.68	0.33	0.47	0.10	0.04	1.10	1.10	0.70	1.60
SCHW-DP-5	70.00	2.48	1.86	0.04	0.59	13.16	0.38	0.66	0.10	0.02	1.20	1.10	0.60	1.60
Average	55.99	2.32	1.48	0.04	0.93	20.58	0.35	0.60	0.10	0.03	1.18	1.20	0.70	1.60

* samples that were resampled.

TABLE DR2. INPUT PARAMETERS FOR THE ^{10}Be MONTE CARLO AGE SIMULATIONS FOR THE SAMPLES IN ÄNGI, RECHBERG, IRCHEL STEIG AND WILEMER IRCHEL (HIDY ET AL., 2010)

Parameter	Ängi	Rechberg	Ircel Steig						
Latitude (degree)	47.560	47.634	47.536						
Longitude (degree)	8.191	8.359	8.615						
Altitude (m)	475	433	675						
Strike (degree)	0	0	0						
Dip (degree)	0	0	0						
Shielding correction factor	1	1	1						
Cover correction factor	1	1	1						
Uncertainty of ^{10}Be Half-life (%)	1	1	1						
Local spallogenic production rate ($\text{at.g}^{-1}.\text{a}^{-1}$)	5.62	5.38	7.05						
Error in local spallogenic production rate ($\text{at.g}^{-1}.\text{a}^{-1}$)	$\pm 0.30 (2\sigma)$	$\pm 0.30 (2\sigma)$	$\pm 0.30 (2\sigma)$						
Error in total production rate (%)	5	5	5						
Density (g.cm^{-3})	1.8 - 2.6	1.8 - 2.6	1.8 - 2.6						
Number of profiles	100'000	100'000	100'000						
Depth of muon fit (m)	155	35	168						
Total erosion threshold (cm)	0 - 15,000	-1000 - 15,000	10,000 - 15,000	0 - 2800	-1000 - 2800	1000 - 2800	0 - 16,000	-1000 - 16,000	10,000 - 16,000
Confidence level (σ)		2			3			2	
Age (a)		0 - 5,000,000			0 - 5,000,000			0 - 5,000,000	
Erosion rate (cm.ka^{-1})		0 - 50			0 - 50			0 - 50	
Inheritance (at.g^{-1})		0 - 30,000			0 - 30,000			0 - 30,000	
Attenuation length (g.cm^{-2})		160 \pm 5			160 \pm 5			160 \pm 5	
Parameter	Wilemer Irchel	Mandach (Akçar et al. 2014)	Stadlerberg (Calude et al. 2017)						
Latitude (degree)	47.545	47.554	47.533						
Longitude (degree)	8.606	8.187	8.446						
Altitude (m)	678	507	610						
Strike (degree)	0	0	0						
Dip (degree)	0	0	0						
Shielding correction factor	1	1	1						
Cover correction factor	1	1	1						
Uncertainty of ^{10}Be Half-life (%)	1	1	1						
Local spallogenic production rate ($\text{at.g}^{-1}.\text{a}^{-1}$)	7.05	5.88	7.18						
Error in local spallogenic production rate ($\text{at.g}^{-1}.\text{a}^{-1}$)	$\pm 0.30 (2\sigma)$	$\pm 0.30 (2\sigma)$	$\pm 0.30 (2\sigma)$						
Error in total production rate (%)	5	5	5						
Density (g.cm^{-3})	2.2 - 2.6	1.8 - 2.6	1.8 - 2.6						
Number of profiles	100'000	100'000	100'000						
Depth of muon fit (m)	157	158	156						
Total erosion threshold (cm)	0 - 15,000	-1000 - 15,000	10,000 - 15,000	0 - 15,000	-1000 - 15,000	10,000 - 15,000	0 - 15,000	-1000 - 15,000	10,000 - 15,000
Confidence level (σ)		4			3			3	
Age (a)		0 - 5,000,000			0 - 5,000,000			0 - 5,000,000	
Erosion rate (cm.ka^{-1})		0 - 50			0 - 50			0 - 50	
Inheritance (at.g^{-1})		0 - 30,000			0 - 30,000			0 - 30,000	
Attenuation length (g.cm^{-2})		160 \pm 5			160 \pm 5			160 \pm 5	

Note: A half-live of 1.387 ± 0.012 Ma for ^{10}Be (Chmeleff et al., 2010; Korschinek et al., 2010) is considered for the calculations. Local spallogenic production rate is calculated with the CRONUS-Earth exposure age calculator (<http://hess.ess.washington.edu/math/>; v. 2.2; Balco et al., 2008 and update from v. 2.1 to v. 2.2 published by Balco in October 2009) and constant production rate Lal (1991)/Stone (2000) scaling model using the NENA (Balco et al., 2009) production rate calibration dataset.

TABLE DR3. INPUT PARAMETERS FOR THE ^{36}Cl MONTE CARLO AGE SIMULATIONS OF THE SAMPLES IN RECHBERG

Parameter	Value
Latitude (degree)	47.634
Longitude (degree)	8.359
Altitude (m)	433
Strike (degree)	0
Dip (degree)	0
Shielding correction factor	1
Cover correction factor	1
Density (g/cm ³)	1.8 - 2.6
Depth of muon fit (m)	20
Scaling scheme (Balco et al., 2008)	St
Spallogenic production rates (at/g/a) from:	
- Ca (Stone et al., 1996)	48.8 ± 3.4
- K (Evans et al., 1997)	170 ± 27
- Ti (Fink et al., 2000)	13 ± 3
- Fe (Stone et al., 2005)	1.9 ± 0.2
Production rate of epithermal neutrons (g air) ⁻¹ a ⁻¹ (Alfimov and Ivy-Ochs, 2009)	760 ± 150
Muogenic production rate error (%)	5
Attenuation length (g/cm ²):	
- fast neutrons	160 ± 8
- epithermal neutrons	3.13 ± 0.25
- thermal neutrons	15.48 ± 1.1
Uncertainty of ^{36}Cl half-life (%)	5
Age (a)	0 - 1,000,000
Net erosion (cm)	0 - 1,300
Erosion rate (cm/ka)	0 - 10
Inheritance (at/g)	0 - 400,000
Confidence interval (σ)	4
Number of profiles	100,000

Note: A half-live (3.013 ± 0.015) $\times 10^5$ a (Lederer and Shirley, 1978) is considered for the calculations

TABLE DR5. RESULTS OF ISOCHRON BURIAL AGE SIMULATION
FOR IRCHEL HÜTZ AND IRCHEL STEIG

Sample name	Measured ^{10}Be (10^3 atoms/g)	Measured ^{26}Al (10^3 atoms/g)	Inherited ^{10}Be concentration (10^3 atoms/g)	^{10}Be linearization factor	Linearized ^{10}Be (10^3 atoms/g)	Age (Ma)
<u>Irchel Hütz</u>						
IRCH-1	7.91 ± 1.27	3.66 ± 0.40	2.09	0.9994	7.84 ± 1.27	
IRCH-5	7.49 ± 0.92	5.00 ± 0.39	1.72	0.9970	7.44 ± 0.92	0.6 ± 0.1 Ma (ratio 6.75)
IRCH-6	7.29 ± 1.09	4.51 ± 0.41	1.49	0.9968	7.23 ± 1.09	0.9 ± 0.4 Ma (ratio 7.6 ± 0.8)
IRCH-8	7.43 ± 1.13	4.17 ± 0.48	1.62	1.0000	7.37 ± 1.13	1.1 ± 0.1 Ma (ratio 8.4)
IRCH-9	12.06 ± 1.18	6.17 ± 0.52	6.25	0.9994	11.99 ± 1.18	
<u>Irchel Steig</u>						
IRCH-10	9.49 ± 1.22	74.32 ± 6.68	1.84	0.9998	9.50 ± 1.22	
IRCH-11	7.63 ± 1.08	64.48 ± 6.08	0.00	1.0000	7.64 ± 1.08	
IRCH-13	9.98 ± 1.23	72.04 ± 6.20	2.33	0.9998	10.00 ± 1.23	
IRCH-14	8.41 ± 1.36	67.49 ± 5.13	0.75	0.9999	8.42 ± 1.36	0.7 ± 0.2 Ma (ratio 6.75)
IRCH-16	14.17 ± 1.54	78.13 ± 6.54	6.48	0.9993	14.18 ± 1.54	0.9 ± 0.4 Ma (ratio 7.6 ± 0.8)
IRCH-17	12.75 ± 1.36	106.74 ± 6.83	5.08	0.9995	12.75 ± 1.36	1.1 ± 0.2 Ma (ratio 8.4)
IRCH-20	13.24 ± 1.43	97.86 ± 7.63	5.57	0.9994	13.25 ± 1.43	
IRCH-21	27.35 ± 2.35	145.99 ± 9.34	19.57	0.9980	27.32 ± 2.35	
IRCH-22	13.95 ± 1.60	100.26 ± 6.52	6.26	0.9994	13.96 ± 1.60	